Experimental Eye Research 127 (2014) 224–235

Contents lists available at ScienceDirect

Experimental Eye Research

journal homepage: www.elsevier.com/locate/yexer

Biomechanical strain as a trigger for pore formation in Schlemm's canal endothelial cells☆

Sietse T. Braakman [a], Ryan M. Pedrigi [a], A. Thomas Read [b], James A.E. Smith [a], W. Daniel Stamer [d], C. Ross Ethier [a, c], Darryl R. Overby [a, *]

[a] Department of Bioengineering, Imperial College London, London, United Kingdom
[b] Department of Ophthalmology and Vision Sciences, University of Toronto, Canada
[c] Coulter Department of Biomedical Engineering, Georgia Institute of Technology and Emory University, USA
[d] Department of Ophthalmology, Duke University Medical School, USA

ARTICLE INFO

Article history:
Received 14 March 2014
Accepted in revised form 5 August 2014
Available online 14 August 2014

Keywords:
Schlemm's canal endothelium
pore
stretch
strain
endothelium
biomechanics

ABSTRACT

The bulk of aqueous humor passing through the conventional outflow pathway must cross the inner wall endothelium of Schlemm's canal (SC), likely through micron-sized transendothelial pores. SC pore density is reduced in glaucoma, possibly contributing to obstructed aqueous humor outflow and elevated intraocular pressure (IOP). Little is known about the mechanisms of pore formation; however, pores are often observed near dome-like cellular outpouchings known as *giant vacuoles* (GVs) where significant biomechanical strain acts on SC cells. We hypothesize that biomechanical strain triggers pore formation in SC cells. To test this hypothesis, primary human SC cells were isolated from three non-glaucomatous donors (aged 34, 44 and 68), and seeded on collagen-coated elastic membranes held within a membrane stretching device. Membranes were then exposed to 0%, 10% or 20% equibiaxial strain, and the cells were aldehyde-fixed 5 min after the onset of strain. Each membrane contained 3-4 separate monolayers of SC cells as replicates ($N = 34$ total monolayers), and pores were assessed by scanning electron microscopy in 12 randomly selected regions (~65,000 μm^2 per monolayer). Pores were identified and counted by four independent masked observers. Pore density increased with strain in all three cell lines ($p < 0.010$), increasing from 87 ± 36 pores/mm^2 at 0% strain to 342 ± 71 at 10% strain; two of the three cell lines showed no additional increase in pore density beyond 10% strain. Transcellular "I-pores" and paracellular "B-pores" both increased with strain ($p < 0.038$), however B-pores represented the majority (76%) of pores. Pore diameter, in contrast, appeared unaffected by strain ($p = 0.25$), having a mean diameter of 0.40 μm for I-pores ($N = 79$ pores) and 0.67 μm for B-pores ($N = 350$ pores). Pore formation appears to be a mechanosensitive process that is triggered by biomechanical strain, suggesting that SC cells have the ability to modulate local pore density and filtration characteristics of the inner wall endothelium based on local biomechanical cues. The molecular mechanisms of pore formation and how they become altered in glaucoma may be studied in vitro using stretched SC cells.

1. Introduction

The endothelium lining the inner wall of Schlemm's canal (SC) contains micron-sized pores that are putative pathways for aqueous humor outflow across an otherwise continuous cell layer containing tight junctions. Pores may pass transcellularly through individual cells (known as "I-pores") or paracellularly through borders between neighboring cells (known as "B-pores") (Epstein and Rohen, 1991; Ethier et al., 1998). The density of I- and B-pores is reduced in primary open angle glaucoma (POAG) (Allingham et al., 1992; Johnson et al., 2002), leading to the possibility that impaired pore formation may contribute to obstruction of aqueous humor drainage through the conventional outflow pathway. Very little is known, however, about the mechanisms of pore formation or the factors that determine pore diameter and density within the inner wall of SC.

SC endothelium experiences significant biomechanical loads due to the basal-to-apical (backwards) direction of aqueous humor

☆ Support: A grant from National Glaucoma Research, (G2009-032) a Program of The BrightFocus Foundation (Formerly the American Health Assistance Foundation), and the National Eye Institute (EY019696).

* Corresponding author. Department of Bioengineering, Imperial College London, London SW7 2AZ, United Kingdom. Tel.: +44 (0) 20 7594 6376.
E-mail address: d.overby@imperial.ac.uk (D.R. Overby).

http://dx.doi.org/10.1016/j.exer.2014.08.003
0014-4835/

flow and pressure drop across the inner wall (Ethier, 2002; Overby et al., 2009). The direction of this pressure drop pushes SC cells away from their underlying basement membrane and the supporting juxtacanalicular tissue (JCT). As a result, SC cells form large dome-like outpouchings, known as *giant vacuoles* (GVs) (Tripathi, 1972; Johnstone and Grant, 1973; Pedrigi et al., 2011), where the instantaneous biomechanical strain acting on SC cells may exceed 50% (Ethier, 2002; Overby, 2011). Pores are often associated with giant vacuoles, and while giant vacuoles and pores are thought to be driven by IOP (Grierson and Lee, 1974, 1977; Lee and Grierson, 1975; Ethier et al., 1998), the precise mechanism of pore formation remains unknown.

We hypothesize that biomechanical strain triggers pore formation in SC cells. To test this hypothesis, SC cells were seeded on elastic membranes that were stretched by 0%, 10% or 20% and aldehyde-fixed in the stretched state. Scanning electron microscopy was used to image SC cell monolayers in order to count pores, measure pore diameter, and classify I- versus B-pores. In vitro pore density and diameter were analyzed as a function of strain, and in vitro pore data were compared against in situ pore data acquired from previous studies of human donor eyes (Ethier et al., 2006). The imaging, identification and classification of pores were done by masked observers who did not know the identity of the samples nor the magnitude of applied strain until after the pore classification was finalized.

2. Methods

2.1. SC cell isolation and culture

This study examined 3 primary SC cell "lines" from non-glaucomatous human donors, aged 34 (SC58), 44 (SC67) and 68 (SC65) years. SC cells were isolated using the cannulation technique of Stamer et al. (1998) and characterized based on expression of VE-cadherin and fibulin-2 (Perkumas and Stamer, 2012). SC cells between passage 3 and 5 were used for all experiments. Although primary cell lines are typically referred to as cell "strains", we refer to these as cell "lines" to avoid confusion with the mechanical "strain" applied to the cells.

Cells were cultured in low glucose DMEM containing 25 mM HEPES buffer (Gibco 12320, Life Technologies Co, USA), 10% fetal bovine serum (Hyclone SH30070.03, Thermo Scientific, USA), 100 U/mL penicillin and 100 μg/mL streptomycin (P4333, Sigma Aldrich, UK). SC cells were cultured in 5% CO_2 in a humid incubator at 37 °C, and passaged prior to confluence using trypsin-EDTA (T4049 Sigma–Aldrich, UK).

2.2. Membrane stretching device

Three membrane stretching devices were machined based on the design of Lee et al. (1996). Briefly, these devices use a coaxial arrangement of threaded cylinders to pull an elastic membrane over an annular indenter (Fig. 1A), thereby imposing equibiaxial strain (i.e., a strain magnitude that is equal in all directions (Ethier and Simmons, 2007)) to the membrane when the outer cylinder is turned with respect to the inner cylinder. The cells were seeded on the upward-facing surface of the membrane, and the membrane and inner cylinder delineate a compartment to hold culture medium. The devices were autoclaved prior to use, and each stretching device was kept sterile after cell seeding by covering it with a lid from a 100 mm plastic petri dish.

To confirm that the membrane strain was equibiaxial and to account for subtle machining variations between devices, each stretching device was calibrated by measuring the two-dimensional Green–Lagrange strain tensor (**E**) as a function of the number of turns of the coaxial cylinders. **E** is a mathematical

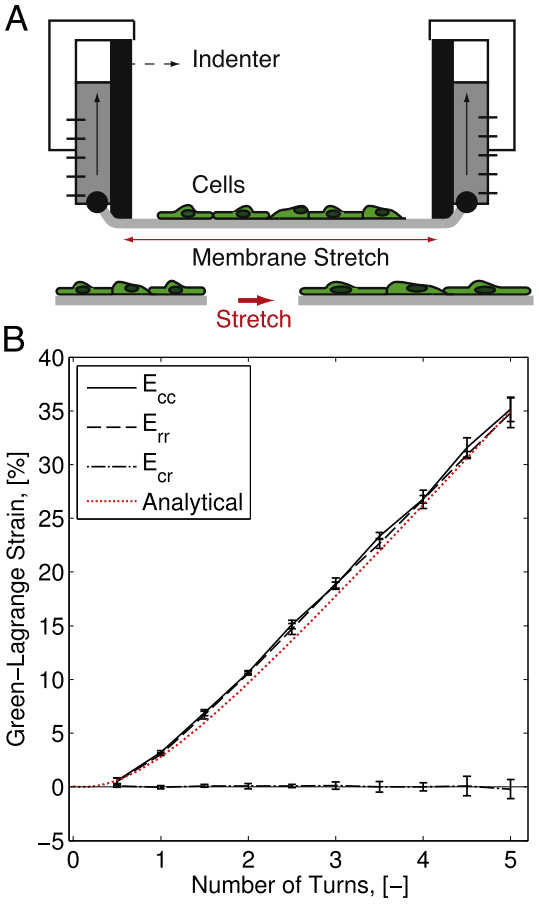

Fig. 1. The membrane stretching device used to apply equibiaxial strain to adherent Schlemm's canal endothelial cells. **A)** A schematic vertical cross-section through the device originally described by Lee et al. (1996). A silicone elastic membrane is clamped into the device and cells are seeded on the upward-facing surface of the membrane. The membrane is stretched by turning the threaded membrane holder (gray) along the outer cylinder (white), thereby pulling the membrane over the indenter (black) to impose equibiaxial strain. **B)** A representative calibration curve obtained from one of the three cell stretching devices used in this study. The measured components of the Green–Lagrange strain tensor (E_{cc}, E_{rr}, E_{cr}) are plotted against the number of turns of the membrane stretching device. The normal components of the strain tensor in the circumferential (E_{cc}) and radial (E_{rr}) directions increase with each turn and remain statistically identical, whereas the shear component (E_{cr}) remains close to zero, indicating that equibiaxial strain is applied to the membrane. The calibration closely follows the analytical solution (Appendix A). Error bars show the standard deviation of each strain component measured over 5 different regions on the membrane.

construct that captures the finite strain (or relative elongation) occurring in each coordinate direction at each point on a membrane undergoing a large deformation ((Humphrey, 2002); see Appendix A). To measure **E**, a grid of 12 fiducial markers was drawn on the membrane (Supplemental Fig. A.1A), and the displacement of these markers was recorded using a CCD camera in steps of ~0.5 whole turns. **E** was then calculated for each set of 4 neighboring markers based on the change in length of the 6 line segments connecting these 4 markers according to.

$$\left(\vec{\delta_{ij}}\right)^2 - \left(\vec{\delta_{ij,0}}\right)^2 = \left(\vec{\delta_{ij,0}}\right)\cdot 2\boldsymbol{E}\cdot\left(\vec{\delta_{ij,0}}\right) \tag{1}$$

where $\vec{\delta_{ij}}$ and $\vec{\delta_{ij,0}}$ are the vectors describing the line segments between markers i and j ($i \neq j$) in the deformed and undeformed states, respectively, expressed in polar coordinates with respect to